Wakefields in the Beamline of TTF Injector II

Ch.X. Tang* and Johnny Ng
DESY, Notkestr. 85, 22607 Hamburg, Germany.

May 28, 1997

Abstract

The results of wakefield calculations for a collection of beamline elements in the TTF Injector II are presented. These elements include crosses, bellows, steps, valves and the bunch compressor. Methods to reduce the wakefield effects due to these elements are also investigated.

TESLA Report 97-11

1 Introduction

A small energy spread and a small transverse emittance are of great importance to achieving high luminosity in linear colliders, and high gain in single-pass X-ray FELs. The Injector II is a photo-cathode RF gun electron injector system for the TESLA Test Facility at DESY. The Injector II beamline contains components such as bellows, steps, crosses, valves, the bunch compressor as well as RF cavities, which give rise to discontinuities in the beam pipe. As the beam traverses these discontinuities, wakefields are excited which cause energy spread and emittance growth. In this report, the results of a study on the wakefield effects of some auxiliary beamline elements in the Injector II are presented.

There are many detailed discussions on wakefield calculations [1, 2, 3, 4]. Here we summarize some concepts relevant to our discussion. The wake function (in Volts/Coulomb) for a bunch traversing a structure parallel to the z axis with an offset (x, y) and at the speed of light is

$$\vec{W}(x,y,s) = -\frac{1}{q}\int_{-\infty}^{+\infty} dz \cdot [\vec{E}(x,y,z,t) + c\vec{e}_z \times \vec{B}(x,y,z,t)]_{t=(s+z)/c} \tag{1}$$

where q is the bunch charge and s is a distance measured from the head towards the tail of the bunch. If we decompose the wake function as: $\vec{W} = \hat{z}W_{//} + \vec{W}_\perp$, the total loss factor of the bunch is given by

$$k_{//}[V/C] = \frac{1}{q}\int_{-\infty}^{+\infty} ds \cdot W_{//}(x,y,s) \cdot \lambda(s) \tag{2}$$

and the transverse impulse factor is,

$$\vec{k}_\perp[V/C] = \frac{1}{q}\int_{-\infty}^{+\infty} ds \cdot \vec{W}_\perp(x,y,s) \cdot \lambda(s) \tag{3}$$

where $\lambda(s)$ is the bunch charge distribution function, and $\frac{1}{q}\int_{-\infty}^{+\infty} ds \cdot \lambda(s) = 1$. The results on transverse impulse factor are presented in this paper in terms of k_x and k_y for non-axisymmetric structures, and k_r for axisymmetric structures. These are normalized to the offset and given in

*Visiting from Department of Engineering Physics, Tsinghua University, Beijing (100084), P.R.China.

units of Volts/Coulomb/meter. A Gaussian bunch is assumed for all the calculations below, that is,

$$\lambda(s) = \frac{1}{\sqrt{2\pi}\cdot\sigma}\cdot e^{-\frac{s^2}{2\sigma^2}}, \tag{4}$$

where σ is the bunch length.

The energy spread caused by wakefield effect is given by $\delta_E = \sqrt{< (E(s) - < E >)^2 >}$, where $E(s) = E_0 + eq\cdot W_{//}(s)$ and E_0 is the initial electron energy of the bunch, and e the unit electric charge. Here "<>" means average over the bunch distribution. The energy spread induced by wakefields is then given by [5]

$$\delta_E = eq\cdot\sqrt{\left[\int_{-\infty}^{+\infty} ds\cdot\lambda(s)\cdot W_{//}^2(s)\right] - k_{//}^2} \tag{5}$$

The results on energy spread presented here are normalized to the bunch charge: $\sigma_E = \delta_E/eq$ in units of Volts/Coulomb. Similarly, the angular divergence caused by transverse wakefields is given by,

$$\delta_\theta = eq\cdot\sqrt{\left[\int_{-\infty}^{+\infty} ds\cdot\lambda(s)\cdot|\vec{W}_\perp(s)|^2\right] - |\vec{k}_\perp|^2} \tag{6}$$

The results are also normalized to the bunch charge and the offset (Δx): $\sigma_\theta = \delta_\theta/(e\cdot q\cdot\Delta x)$ in units of radians·Volts/Coulomb/m. In order to obtain the emittance growth from σ_θ, the beam transport optics must be taken into account [4]. There are also additional effects such as space charge force which also lead to emittance growth [6].

2 Wakefield calculations

ABCI [7] and MAFIA [8, 1] are the two commonly used codes for numerical wakefield calculations. In this paper, the axisymmetric structures, like bellows and steps, are calculated with ABCI, and the crosses with MAFIA. The reliability of both codes are investigated here.

Comparison of ABCI with measurement. Tab.1 shows the calculation results of ABCI compared with the measured values for the CESR copper cavity [9]. The results are satisfactory, and give an estimate of the reliability of the calculations.

Table 1: Comparison of ABCI calculation with measured values for a CESR cavity.

parameter	measured	ABCI	error
$k_{//}$(V/pC)(HOM)	0.34	0.32	<10%
R/Q(Ω/cell)(fundamental)	265	306	<15%

3D wakefield calculation with MAFIA. Wakefield calculation for a 3D structure with MAFIA is investigated here. Usually, only a quarter of the structure is meshed. In this case, the modes m=1,3,5,... cannot be excited if the lower boundary conditions of x and y directions are magnetic; while the modes m=0,2,4,... cannot be excited if one of the lower boundary conditions of x and y directions is magnetic, and the other one is electric. Therefore, two calculations with the beam traveling at an offset from the z-axis are required. The wakefields for a 6-port cross CF35 are computed for the whole and for a quarter of the structure. The results are given in Tab.2 and they agree very well.

Table 2: Wakefield calculation for 3D structures with MAFIA. (Note the results for k_y has not be normalized to the offset here.) Results of calculations using a quarter or the complete structure are shown for comparison.

y offset(mm)	4	8	12	16
$k_{//}$(V/pC),whole	-0.489	-0.6300	-0.950	-1.600
$k_{//}$(V/pC),a quarter	-0.489	-0.6304	-0.954	-1.599
k_y(V/pC),whole	-0.0930	-0.2480	-0.5820	-1.560
k_y(V/pC),a quarter	-0.0933	-0.2475	-0.5815	-1.564

Comparison of MAFIA with ABCI. Comparison between the wakefield calculations of MAFIA(T2) and ABCI for a pillbox is shown in Tab.3. The maximum difference for a very short bunch is within 5%. For structures with beam tubes of different size and shape at both ends, the results from these two codes depend on the details in the calculation. Results for the step transition is given in section 3.3.

Table 3: Comparison between MAFIA and ABCI for a pill-box cavity.

σ(mm)	2.0		0.2	
code	MAFIA	ABCI	MAFIA	ABCI
$k_{//}$(V/pC)	-0.872	-0.875	-3.023	-3.175
$k_{\perp}$(V/pC/m)	15.52	15.74	5.564	5.661
σ_E(V/pC)	0.339	0.335	1.261	1.240

3 Results for Injector II Beamline Elements

3.1 Crosses

Here three kinds of crosses in the beamline of injector II are considered: a 6-port cross, a 4-port cross, and a 10-port cross which consists of two 6-port crosses connected together. (A 6 port has 4 ports plus 2 ports for beam tube connection.) These ports are used for pumping or beam diagnostics, but also lead to discontinuities in the vacuum chamber. The wakefield effects for various crosses are summarized in Tab.6.

The wakefield effects are studied as a function of the diameters of the 6- and 4-port crosses, and the resulting least-squares fit parametrizations are given in Tab.5. The longitudinal wake potential for different diameters are shown in Fig.1 for a 6-port cross for bunch length $\sigma = 2.0$ mm.

One of the 10-port crosses under study consists of two 6-port crosses of different diameters. Tubes of equal diameter are added to both ends of the 10-port cross so that the indirect method of MAFIA can be used during the wakefields calculation. The beam tube diameter at both ends is 35 mm. For one of the 6-port, all port diameters are 48 mm. For the other 6-port, 3 of the ports have a diameter of 63 mm, and 2 of the ports 100 mm. The port connecting the two crosses has a diameter of 48 mm. So the structure includes a step transition from 35 mm to 48 mm at one end and a transition from 63 mm to 35 mm at the other end. The loss factors and transverse impulse factors for this 10-port are much larger than those for the 6-port and 4-port crosses. Another 10-port cross under study consists of two 6-port crosses with the same diameters of 35 mm for all ports. Its wakefield effects are smaller than the one with different diameters.

Shielding plates can be used to reduce the wakefield effects in the crosses. Some designs of shielding plates consisting of a mesh of metal bars are investigated in ref. [10]. When the direction of the metal bars is along the beam direction, the energy loss factor decreases rapidly as the width

of the metal bars are reduced. However, if the direction of the metal bars is perpendicular to the beam direction, there is almost no reduction in the wakefield effects.

3.2 Bellows

Two kinds of bellows are investigated in this section, one with circular and the other with triangular convolutions. The wakefield effects calculated with ABCI are summarized in Tab.6.

The C5-13-8 bellow is shown in Fig.2. It has 8 circular convolutions, with a total height of 13 mm, and a bending diameter of 5 mm. The separation between each convolution is 10 mm. The longitudinal and transverse wakefield effects for different bunch length are given in Tab. 6. The loss factor and energy spread vary linearly with the number of convolutions of the bellow.

The wakefield effects of bellows can be reduced with shielding. Here, the bellow is simply shielded with a cookie-cutter: a cylindrical shell underneath the bellow. The reduction in energy spread is by a factor of 2, for σ=0.8 mm, and by a factor of 10 for σ=10 mm. But it also depends on the distance between the shield and the bellow beam tube. The loss factor and energy spread for bellow C5-13-8 with cookie-cutter are shown in Fig.3 with and without shielding, as a function of bunch length, and in Fig.4 as a function of the distance of the shield to the beam axis. A thickness of 1 mm is used for the shield. The length of the shield covers completely the bellow.

3.3 Step transition with and without taper

The steps in the beam pipe of injector II are mainly step-out D35–D63(diameter changes from 35 mm to 63 mm without taper) and step-in D63–D35. Results calculated using ABCI for the steps between D64 and D36 are given here. Napoly's integration method [11] is employed in ABCI to calculate the wakefield effects of a structure with beam pipes of different diameters at both ends. Fig.5 shows the loss factors for step-out and step-in between D=36mm and D=64mm calculated using ABCI as a function of bunch length. The loss factor for step-in is nearly zero but negative. The energy gain is due to the attractive force of the image charge [2]. Also shown in Fig.5 are the loss factors calculated using MAFIA at a bunch length of 5.0 mm. The results are similar to those obtained using ABCI. The difference between the energy spreads calculated using these two codes at the bunch length of 5.0 mm is approximately 30% for both step-in and step-out.

The wake functions of step-in and step-out calculated using ABCI are shown in Fig. 6. The LOG term in the output of ABCI comes from the difference of the potential energies of the electromagnetic fields surrounding the beam in the two beam pipes at both ends [7, 11]. The wake functions of step-in and step-out are almost the same if the LOG term is not included.

Fig. 7 shows the configuration for step-out and step-in with a taper, where θ is the angle of the taper. The loss factors and energy spreads of a tapered step are shown in Fig.8 and Fig.9, respectively, as a function of the taper angle θ for 1 mm bunch length. For tapered step-in and step-out, the loss factors decrease while the energy spreads increase as the taper becomes more gradual. Therefore, a gradual tapered step transition reduces the loss factor, but at the cost of increasing the energy spread.

To study any dependence on the mesh size in ABCI, the calculations were repeated with different mesh sizes. The results are shown in Fig. 10 for a bunch length of 1 mm in step transitions with and without taper. The variations of the calculated loss factor and energy spread become reasonably small when the mesh size is smaller than the bunch length by at least a factor of 20. The results presented in this section were calculated with a mesh size which is a factor 50 smaller than the bunch length.

3.4 Valves

Valves in the beamline of injector II are used to isolate the vacuum in one section of the beamline from the vacuum of the adjacent section. A valve in the beamline is like a rectangular cavity when it is open. The structure of the valve used in the calculation is simplified as shown in Fig. 11 with a square cross-section and a gap of 25mm. Because the indirect method in MAFIA is used here,

Table 4: The loss factor, energy spread and transverse impulse factor are parametrized linearly as a function of the bunch compressor chamber boundary curvature radius (R) by $a + b \cdot R$, where R is in mm. The parameters a and b are given here.

σ (mm)	loss factor (V/pC)		energy spread (KV/nC)		transverse impulse factor (V/pC/m)	
	a	b	a	b	a	b
0.8	2.361	0.00196	1.195	0.00270		
1.2	1.840	0.00176	1.023	0.00230	82.42	0.0483
2.0	0.858	0.000201	0.626	0.00072		
3.5	0.325	0.000117	0.326	-0.000022		
5.0	0.159	0.000080	0.201	0.000019		

the lengthes of the beam pipes at both ends almost have no influence on the wakefields calculation results [1].

The loss factor of a valve with a diameter of 63mm as a function of the width of the rectangular cavity for different bunch length is given in Fig.12, which shows that the loss factors are almost constant when the width of the square cavity changes from 85mm to 150mm. Similar behaviour is obtained for the energy spread.

The transverse wakefields are also studied for a valve with D=63mm and width=112mm at the offset point $x = 2$ mm, $y = 0$ (along the x-axis) and the offset point $x = 2$ mm, $y = 2$ mm (along the diagonal) for different bunch lengthes. The results are shown in Fig. 13.

3.5 Bunch compressor

The bunch compressor for Injector II consists of four dipole magnets and a vacuum chamber with complicated geometry. The shape of the chamber in the x-z plane is shown in Fig. 14. The curves of the chamber boundary have a radius of 667.67mm. A cut along the x-y plane at a given z is a rectangle, with a fixed height (along y) of 35 mm. The beam pipes at both ends have a diameter of 35mm.

For long structures, the dispersion error due to finite mesh size (in z) need to be considered during the calculation. With the following condition the dispersion error is suppressed:

$$\frac{\delta_z^2 \cdot L}{\sigma^3} \leq 1 \tag{7}$$

where L is the total length of the structure, δ_z the mesh step in z direction, and σ the bunch length. For a structure with large L, the mesh step in the beam direction should be small.

Because the length of the chamber is large (approximately 1.4 m), the total number of mesh points becomes prohibitively large for bunch lengthes shorter than 1 mm. In the calculation, a chamber with a smaller boundary curvature radius, in the range of 50 mm to 400 mm, is used. The wakefield effects for the Injector II chamber can be obtained by extrapolation, using the the linear fitting parametrizations given in table 4. Also, in the calculation, the beam traverses along a straight line connecting the center of the beam pipes at both ends. Fig. 15 shows the loss factors as a function of the radius of the chamber boundary curve, together with the parametrizations.

4 Summary

The calculations of loss factors, transverse impulse factors, and energy spreads and the angular divergences induced by wakefield effects of some elements of the beamline of Injector II are reported. The calculated results are summarized in Tab.6. These results can serve as a guide when selecting elements for a beamline where wakefield effects must be taken into account.

Acknowledgement

We wish to thank Y.H. Chin, P. Colestock, M. Dohlus, H. Edwards, K. Floettmann, S. Schreiber, J. Sekutowicz, R. Wanzenburg, and M. Zhang for many useful discussions.

References

[1] T. Weiland, R. Wanzenburg, DESY M-91-06.

[2] S. A. Heifets and S. A. Kheifets, Rev. Mod. Phys. vol. 63, No.3, (1991)631.

[3] L. Palumbo, V. G. Vaccaro, and M. Zobov, LNF-94/041, Lecture at CERN Acc. School, 1994.

[4] K.C.D.Chan, LA-UR-88-2120.

[5] R. Wanzenburg, private communication (1996).

[6] See for example, presentations by M. Zhang and P. Colestock *et al* at the TESLA Collaboration Meeting, March 1997.

[7] Y.H. Chin, CERN SL/94-02(AP).

[8] MAFIA code group.

[9] K. Berkelman *et al.*, CLNS91-1050, and M. Tigner, private communications.

[10] R. Wallace, K.C.D. Chan,NIM A304(1991)400-405.

[11] O. Napoly, Particle Accelerator, Vol.36 (1991)15-23.

Table 5: Least-squares fit parametrizations of wakefield effects for 6- and 4-port crosses as a function of port diameters D in mm for 2 mm bunch length.

	6-port cross	4-port cross
energy spread	$\sigma_E[KV/nC] = 0.319 - 0.00097D + 4.225/D$	$\sigma_E[KV/nC] = 0.196 - 0.00044D - 0.345/D + 39.2/D^2$
loss factor	$k_{//}[V/pC] = 0.989 - 0.0040D + 5.786/D$	$k_{//}[V/pC] = 0.377 - 0.000267D + 7.26/D - 97.7/D^2$
transverse impulse factor	$k_x[V/pC/m] = 13.75 - 0.069D - 998.5/D + 41110/D^2$	$k_x[V/pC/m] = 26.3 - 0.127D - 1940/D + 76000/D^2$
frequency of resonance modes	$f[GHz] = 4.618 - 0.032D - 49.54/D + 2276/D^2$	

Table 6: Wakefield effects for the beamline elements of Injector II for different bunch lengths. Two different diameters are used for the 6- and 4-port crosses. Detailed description for the 10-port is given in the text. The structures of the valve and the bunch compressor are given in Fig. 11 and Fig. 14. Two types of bellows with triangular and circular convolutions, and different number of convolutions and diameters are shown.

element	6-port cross [a]						4-port cross [a]							
description	CF35:D=35mm			CF63:D=63mm			CF35:D=35mm				CF63:D=63mm			
σ(mm)	$k_{//}$ (V/pC)	σ_E (KV/nC)	k_x [b] V/pC/m	$k_{//}$ (V/pC)	σ_E (KV/nC)	k_x [b] V/pC/m	$k_{//}$ (V/pC)	σ_E (KV/nC)	k_x [b] V/pC/m	k_y [b] V/pC/m	$k_{//}$ (V/pC)	σ_E (KV/nC)	k_x [b] V/pC/m	k_y [b] V/pC/m
0.8	1.730		11.75	1.376			1.120	0.434	19.20	10.40	0.921	0.358	4.380	2.730
1.2	1.400		14.20	1.134		3.810	0.796	0.309	22.80	11.80	0.687	0.261	5.300	3.200
1.6	1.170		15.90	0.835										
2.0	0.998	0.412	17.05	0.569	0.324	3.900	0.496	0.203	28.95		0.452	0.173	6.790	
2.4	0.867		17.85	0.431										
2.8	0.762		18.40	0.216										

element	10-port cross [a]								valve [a]				step-out [c]	
description	6-port(D48)+6-port(D63,100)				6-port(CF35)+6-port(CF35)				square cavity:112,D:63,gap:25				D:36–64mm	
σ(mm)	$k_{//}$ (V/pC)	σ_E (KV/nC)	k_x [b] V/pC/m	σ_θ [d] rad·V/pC/m	$k_{//}$ (V/pC)	σ_E (KV/nC)	k_x [b] V/pC/m	σ_θ [d] rad·V/pC/m	$k_{//}$ (V/pC)	σ_E (KV/nC)	k_x [b] V/pC/m	σ_θ [d] rad·V/pC/m	$k_{//}$ (V/pC)	σ_E (KV/nC)
0.8	6.155	3.291	40.50	31.60	3.412	1.426	20.35	17.08	0.929	0.371	2.157	1.470	7.189	2.888
1.2	5.499	2.650	51.75	37.67	2.834	1.197	26.80	21.54	0.745	0.291	2.581	1.834	4.730	1.939
2.0	4.176	1.945	56.90	37.23	2.038	0.812	33.81	24.79	0.556	0.215	3.197	2.277	2.756	1.169
3.5	2.692	1.111	56.10	32.77	1.435	0.566	38.13	25.66	0.397	0.152	3.980	2.859	1.492	0.671
5.0	1.923	0.823	52.90	28.83	0.949	0.431	39.36	23.93	0.318	0.121	4.520	3.202	0.988	0.475

element	step-in [c]		bellow I [c]				bellow II [c]				bunch compressor [a]			
description	D:64–36mm		triangular:N=10,D35mm				circular:N=8,D63mm				flat chamber:r=667.67, D:35			
σ(mm)	$k_{//}$ (V/pC)	σ_E (KV/nC)	$k_{//}$ (V/pC)	σ_E (KV/nC)	k_r V/pC/m	σ_θ rad·V/pC/m	$k_{//}$ (V/pC)	σ_E (KV/nC)	k_r V/pC/m	σ_θ rad·V/pC/m	$k_{//}$ (V/pC)	σ_E (KV/nC)	k_x [b] V/pC/m	σ_θ [d] rad·V/pC/m
0.8			1.382	0.560	10.27	7.824	2.246	0.830	5.186	3.718	3.431	2.431	114.7	119.3
1.2	-.189	0.101	1.118	0.450	12.48	9.439	1.757	0.650	6.041	4.366				
2.0	-.189	0.103	0.761	0.300	15.57	11.39	1.305	0.490	7.371	5.405				
3.5	-.188	0.105	0.490	0.200	18.25	12.28	0.947	0.370	9.314	6.810	0.396	0.953		
5.0	-.183	0.105	0.327	0.180	18.53	11.35	0.745	0.290	10.59	7.523	0.166	0.298		

[a] MAFIA calculation
[b] The transverse impulse factors is only valid near the beam axis.
[c] ABCI calculation. The data of step-in and step-out are those of with LOG term.
[d] The angular divergence is only valid near the beam axis.

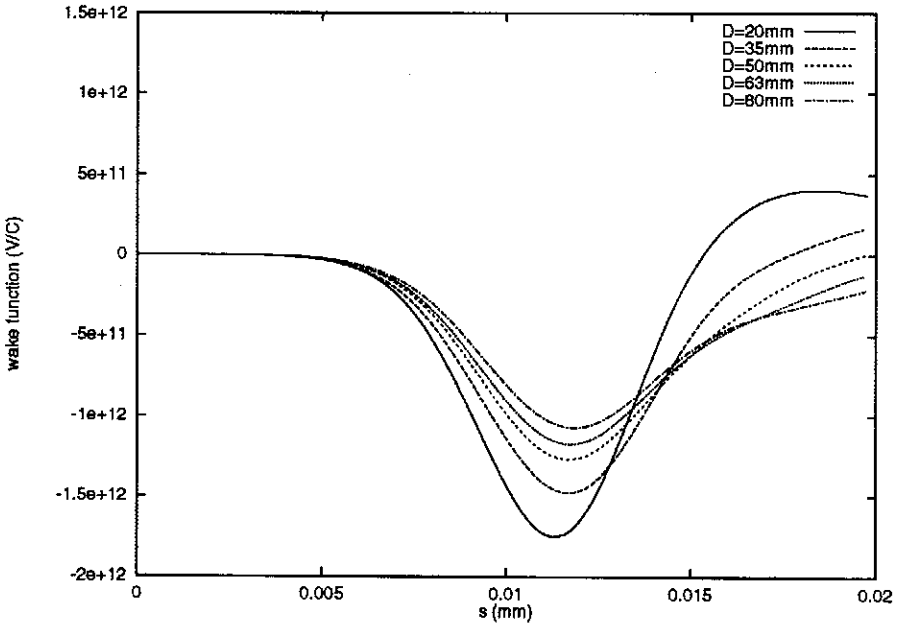

Figure 1: The wake function W_z for 6-port crosses with different diameters for a bunch length of 2 mm.

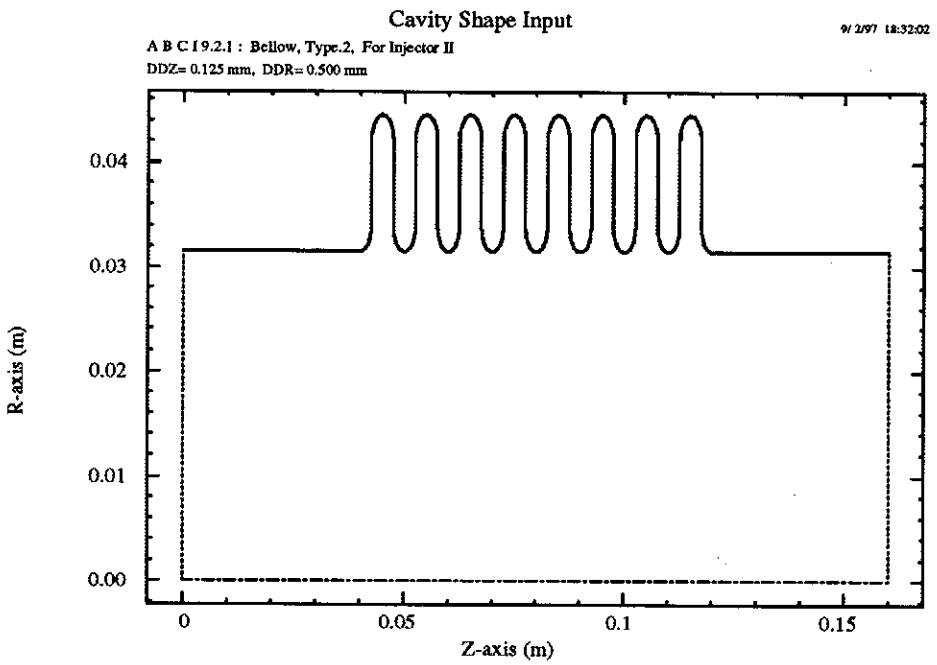

Figure 2: A sketch of the bellow C5-13-8. See text for detailed description.

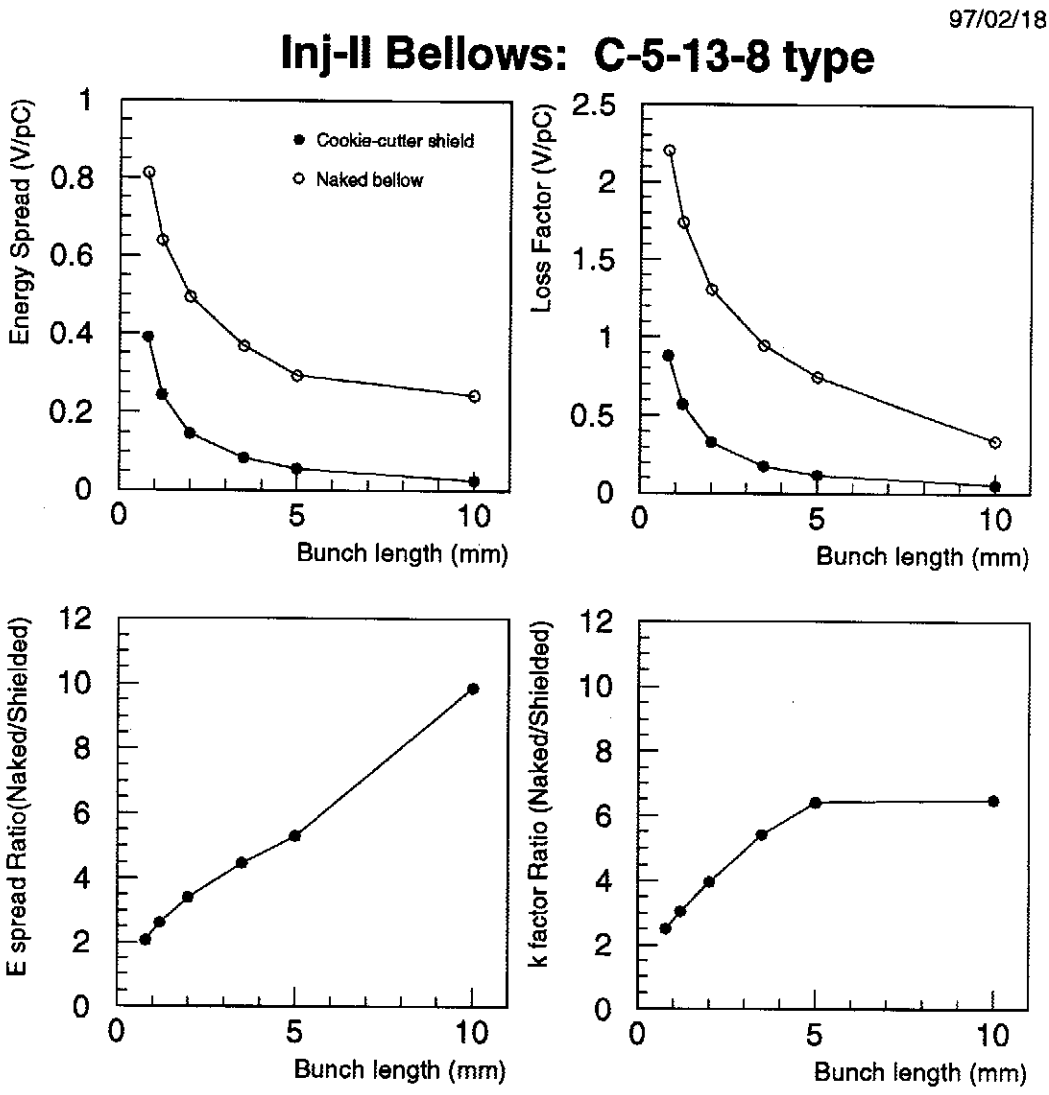

Figure 3: Loss factor and energy spread for bellow C5-13-8 with and without shielding, as a function of bunch length.

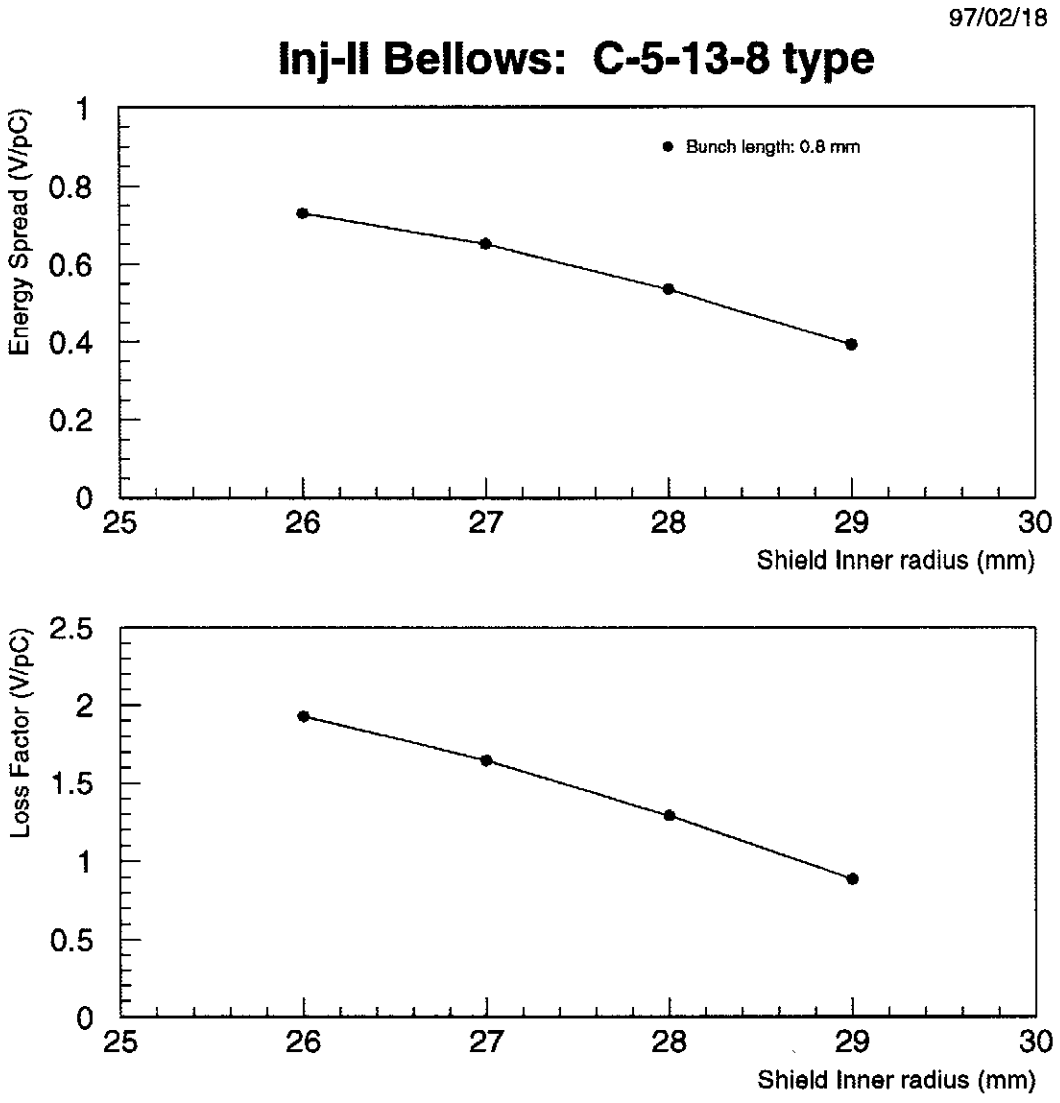

Figure 4: Loss factor and energy spread for bellow C5-13-8 with shielding, as a function of the distance of the shield to the beam axis.

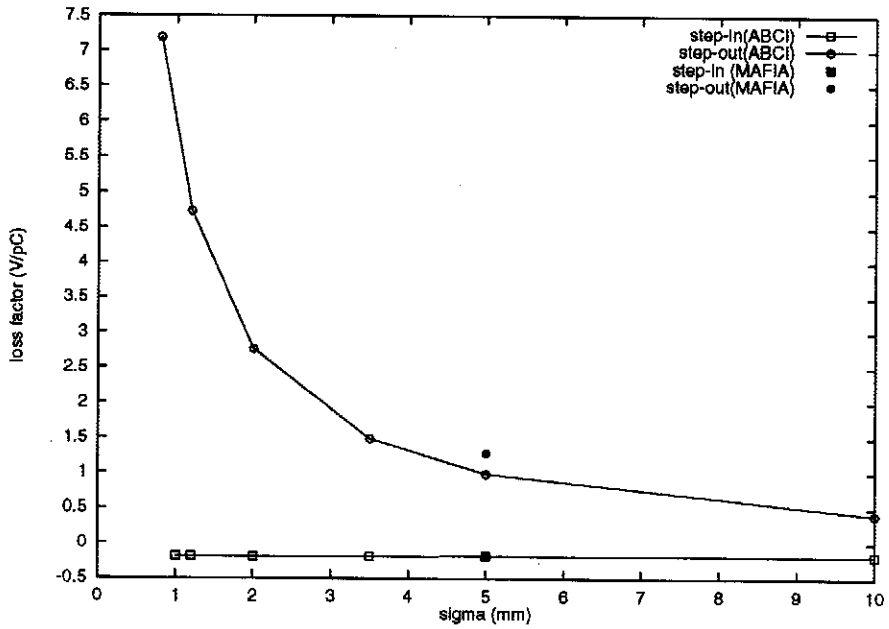

Figure 5: Loss factor for steps as a function of bunch length. Results from ABCI and one point from MAFIA are shown.

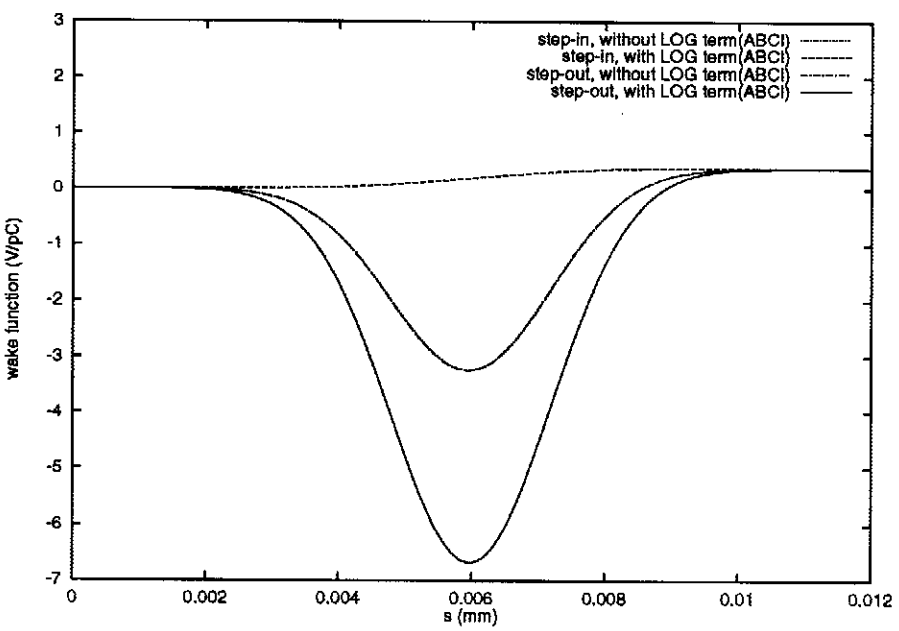

Figure 6: Wake functions of step-in and step-out at bunch length of 1.2mm calculated using ABCI. The results of with and without LOG term are shown.

Figure 7: Configuration of step-in(a) and step-out(b) with taper angle θ.

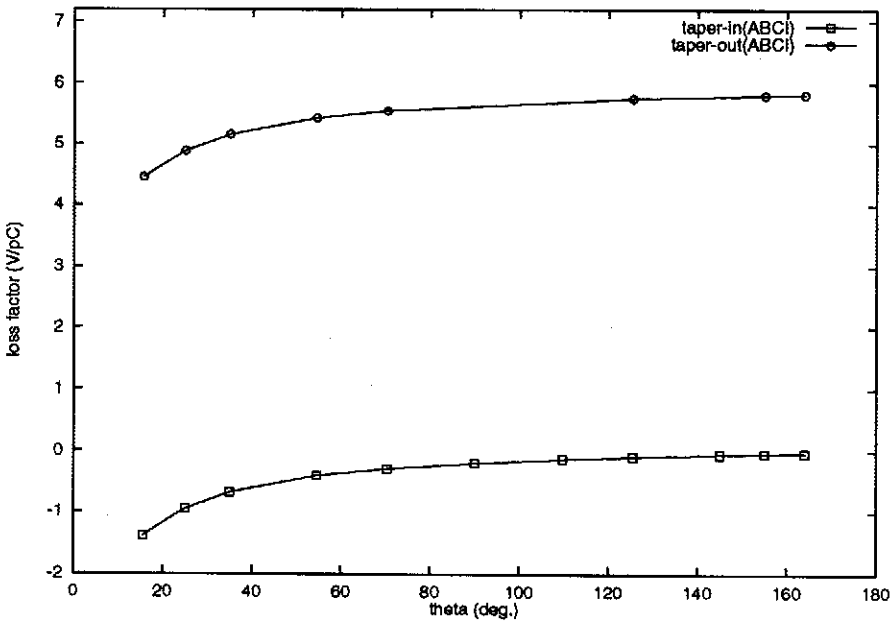

Figure 8: Loss factors as a function of taper angle for 1 mm bunch length.

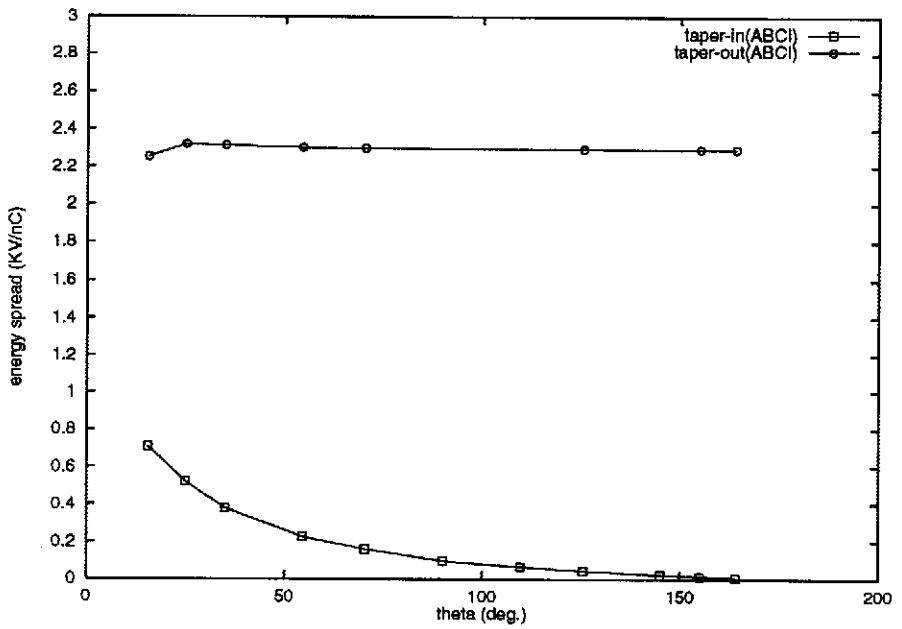

Figure 9: Energy spread as a function of taper angle for 1 mm bunch length.

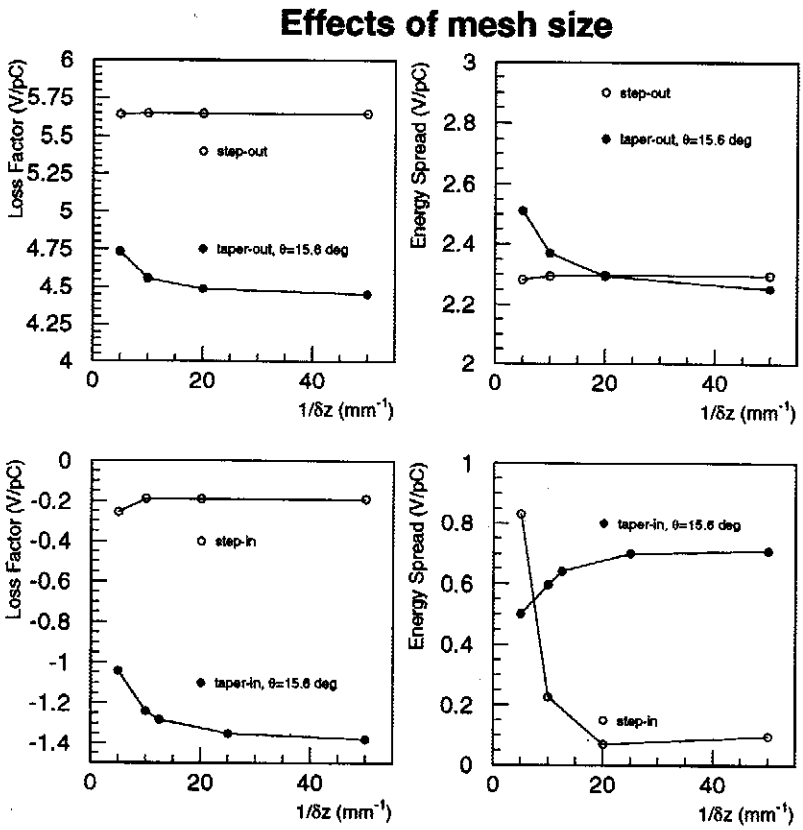

Figure 10: Effects of the mesh size in ABCI for step transitions. The loss factor and energy spread are shown for 1 mm bunch length obtained with various mesh sizes δz.

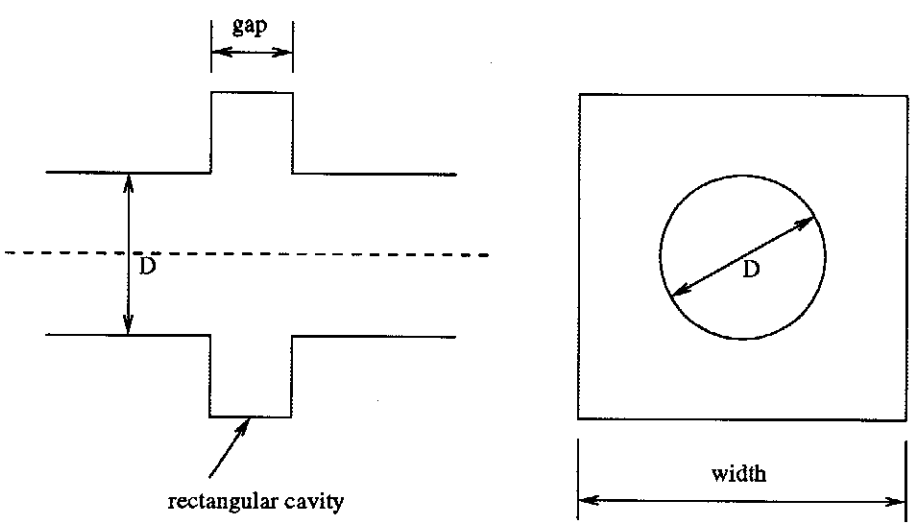

Figure 11: A sketch of the valve used in the calculation.

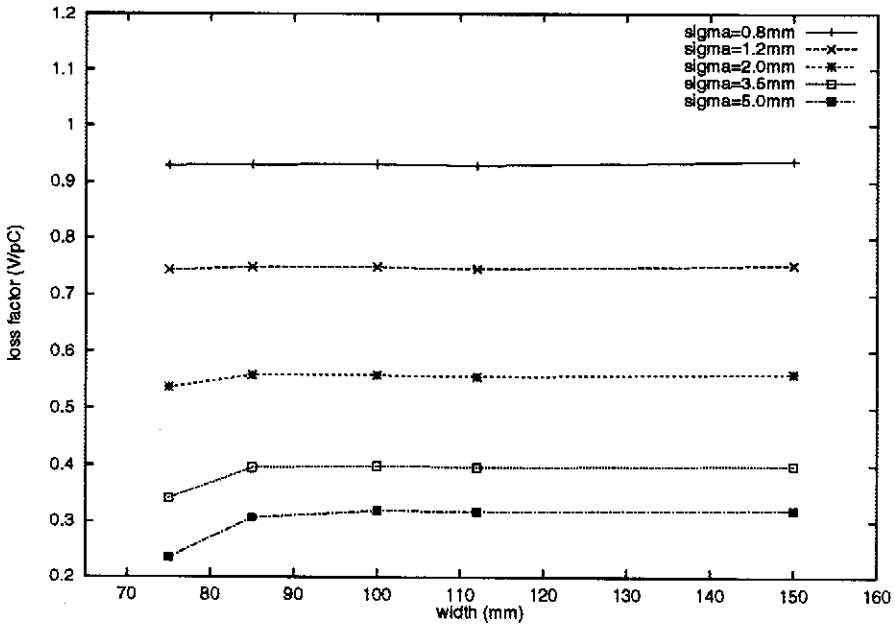

Figure 12: Loss factor of a valve with a beam pipe diameter of 63mm, for different bunch length, as a function of the width for the rectangular cavity.

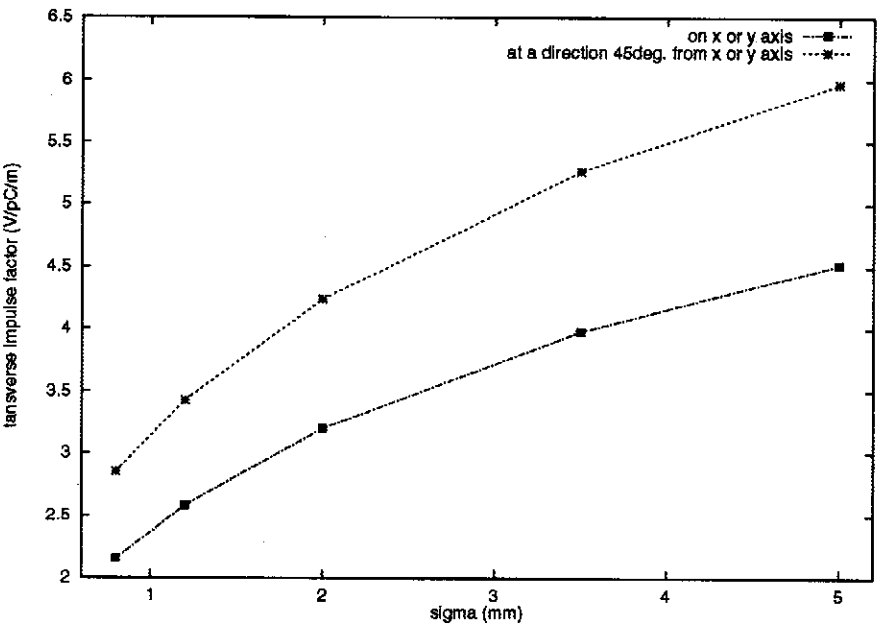

Figure 13: Transverse impulse factor of a valve with beam pipe diameter of 63 mm, width of 112 mm of the rectangular cavity for different offset positions, as a function of the bunch length.

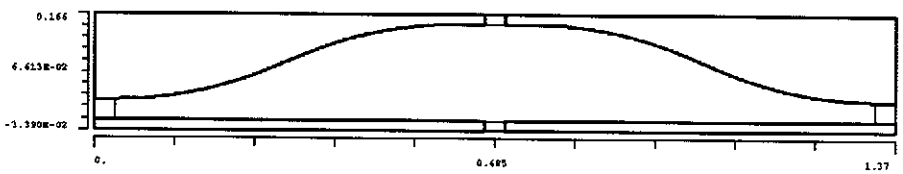

Figure 14: A sketch of the bunch compressor vacuum chamber in the x-z plane.

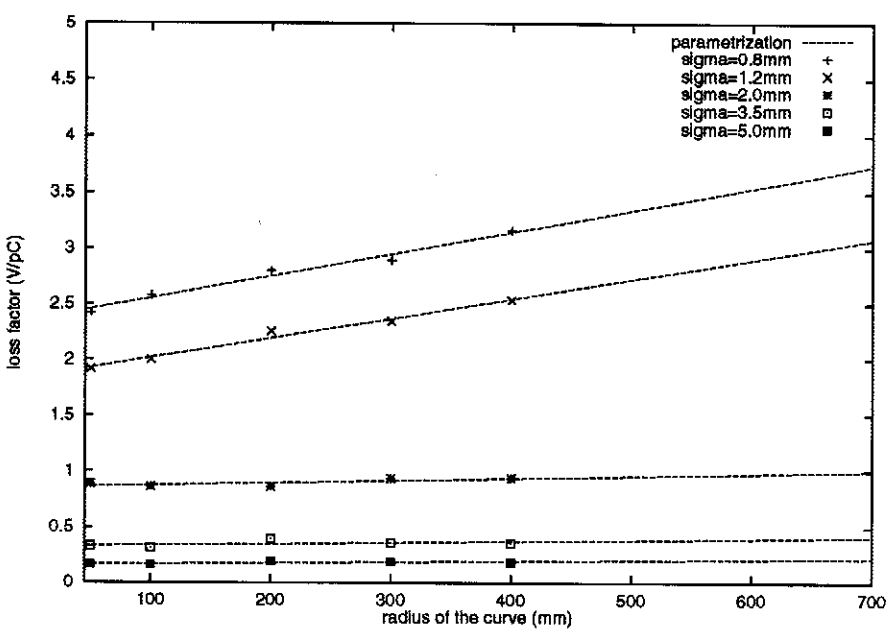

Figure 15: Loss factor for different bunch length, as a function of the curvature radius of the vacuum chamber boundary of the bunch compressor.